

Rate Adaptation using Acknowledgement Feedback in Finite-State Markov Channels with Collisions

Chin Keong Ho, *Member, IEEE*, Job Oostveen, *Member, IEEE*
and Jean-Paul M.G. Linnartz, *Senior Member, IEEE*

Abstract—We investigate packet-by-packet rate adaptation so as to maximize the throughput. We consider a finite-state Markov channel (FSMC) with collisions, which models channel fading as well as collisions due to multi-user interference. To limit the amount of feedback data, we only use past packet acknowledgements (ACKs) and past rates as channel state information. The maximum achievable throughput is computationally prohibitive to determine, thus we employ a two-pronged approach. Firstly, we derive new upper bounds on the maximum achievable throughput, which are tighter than previously known ones. Secondly, we propose the particle-filter-based rate adaptation (PRA), which employs a particle filter to estimate the *a posteriori* channel distribution. The PRA can easily be implemented even when the number of available rates is large. Numerical studies show that the PRA performs within one dB of SNR to the proposed upper bounds for a slowly time-varying channel, even in the presence of multi-user interference.

Index Terms—Rate adaptation, ARQ, particle filter, finite-state Markov channel, dynamic programming.

I. INTRODUCTION

PACKET switching is prevalent in current wireless communication systems, e.g., in wireless LANs based on the IEEE 802.11 standards [1] and in cellular networks with 3G long term evolution (LTE) capabilities [2]. Automatic repeat request (ARQ) [3], [4] is commonly used to enhance the reliability or the throughput of packet-switched systems. When the channel experiences an instantaneous deep fade or is subject to strong interference, a packet cannot be recovered. An explicit negative acknowledgement (NACK), or a missing positive ACK (PACK), is then used to signal a retransmission. To efficiently use the channel, the rate at which each packet is encoded, i.e., the modulation constellation and code rate used, should ideally match the instantaneous channel condition.

Manuscript received March 7, 2008; revised July 28, 2008 and November 11, 2008; accepted December 10, 2008. The associate editor coordinating the review of this letter and approving it for publication was Prof. Q. Zhang.

C. K. Ho is with the Institute for Infocomm Research, A*STAR, Singapore. He conducted part of this work while with the Department of Electrical Engineering, Eindhoven University of Technology and with Philips Research Laboratories, Eindhoven, The Netherlands. (e-mail: hock@i2r.a-star.edu.sg).

J. Oostveen is with TNO Information & Communication Technology, Mobile Networks Department, Groningen, The Netherlands. He conducted part of this work while with Philips Research Laboratories, Eindhoven, The Netherlands. (e-mail: job.oostveen@tno.nl).

J.-P. M. G. Linnartz is with Philips Research Laboratories, Eindhoven, The Netherlands, and with the Department of Electrical Engineering, Eindhoven University of Technology. (e-mail: j.p.linnartz@philips.com).

This work was presented in part at IEEE Vehicular Technology Conference, Melbourne, Australia, May 2006 and at IEEE Globecom, New Orleans, LA, Dec. 2008.

Digital Object Identifier 10.1109/TWC.2009.081009.

This poses a challenging tracking problem for time-varying channels, particularly in the presence of interference.

Tracking the channel and matching to it the rate of the packet is accomplished by *rate adaptation* [5]–[8], known also as adaptive signalling [9], adaptive modulation and coding [10], link adaptation [11]–[15], auto-rate [16] and adaptive error control [17]. To perform rate adaptation, channel state information (CSI) is needed. Although more informative CSI leads to better channel tracking and hence higher throughput, in practice the availability of CSI is limited by the communication scenario and system employed. For example, in IEEE 802.11a/b/g systems, the Request-to-Send/Clear-to-Send (RTS/CTS) mechanism, a handshaking protocol to set up communication, is exploited to assess the channel state in [6] or to differentiate packet collisions from packet failures caused by a deep channel fade in [7], [8]. However, the RTS/CTS mechanism is used only in certain communication systems. Some advanced rate adaptation schemes require more extensive feedback beyond the standard ACK feedback, e.g., [9], [10], and may not be compliant with legacy standards such as IEEE 802.11a/b/g. In frequency division duplex systems, channel reciprocity is often not valid, i.e., the return channel may not behave identically as the forward channel. In such systems, rate adaptation schemes that exploit channel reciprocity for measuring the channel quality of the forward channel, such as [5], [12], [13], cannot be used effectively.

Rate adaptation can be implemented for any ARQ system if only the history of ACKs is used as CSI, such as in [14]–[16], without assuming channel reciprocity and availability of additional CSI. In [14]–[16], the rate of the next packet is increased or decreased *relative* to the previous rate, depending on the number of most recent consecutive PACKs or NACKs received. In [17], [18], besides past ACKs, past rates are also used as CSI. No additional feedback is incurred, since the rates are known at the transmitter and need only to be stored in memory. In [17], the CSI is limited to past rates and ACKs in the same *frame*, where a frame typically consists of several packets. In [18], *all* past rates and ACKs are used as CSI, which improves the tracking of the channel quality; for brevity we refer to this as *ACK-rate CSI*.

The problem of optimally adapting the rate using the ACK-rate CSI so as to maximize the throughput is a PSPACE-complete problem [18], [19], which is considered at least as hard as an NP-complete problem. This means that optimal rate adaptation schemes cannot be computed or implemented practically. Hence, rate adaptation schemes based on heuris-

tics are devised in [18]. However, the complexity of these heuristic schemes can still increase quickly if the number of possible rates becomes large. Since the maximum achievable throughput cannot be computed numerically, a computable upper bound is obtained in [18]. However, this upper bound may not be sufficiently tight in some channels. A tight computable upper bound is desirable since it provides an accurate indication of how close a rate adaptation scheme performs with respect to the optimal one. Moreover, although collisions due to multi-user interference occur frequently in practice, collisions have not been considered in [17], [18]. As such, an overly conservative rate adaptation scheme may result, because an NACK caused by a collision may be wrongly perceived to be caused by a deep channel fade.

In this paper, to match variations in channel conditions, we employ rate adaptation and seek to maximize the throughput averaged over an infinite time horizon. To limit the feedback, ACK-rate CSI is employed. The ACK feedback is used for rate adaptation in IEEE 802.11a/b/g systems. One of the important challenges in wireless system standardization is to keep the amount of channel feedback small. The use of a one-bit feedback (via ACK) represents the extreme case of limited feedback and is thus useful as benchmark for future schemes or other existing schemes that require more feedback.

To obtain tractable results and to build insights, in our analysis we use a first-order finite-state Markov channel (FSMC) to model the channel variation over time [20]. We assume that the buffer for storing information bits at the transmitter has infinite size and always contains sufficient bits. This is appropriate if many information bits are already pre-stored at the transmitter, such as in streaming applications.

Our contribution pertains to these new improved aspects.

- We study the effects of collisions on rate adaptations, by modeling collisions in the FSMC.
- We establish two new computable upper bounds that are tighter than currently known ones. To obtain these upper bounds, we let the transmitter receive a CSI that is more informative than ACK-rate CSI. Specifically, we periodically update the transmitter with a delayed version of the exact channel coefficient, in addition to the ACK-rate CSI.
- We propose practical near-optimum rate adaptation schemes. To reduce the complexity of real-time implementation, we consider the pragmatic approach of maximizing over a sliding, finite time horizon. Further, we propose the *particle-filter-based rate adaptation* (PRA), which employs the particle filter [21] for rate adaptation. The PRA has a complexity that is largely independent of the number of rates used. This allows us to use a large number of rates when we explore the potential of rate adaptation.

For simplicity in obtaining numerical results, we assume that a packet is erroneous if the SNR is less than a rate-dependent threshold or if a collision occurs. Our numerical studies show that the throughput performance drops drastically if collisions are not properly accounted for. Moreover, the proposed PRA outperforms conventional schemes and performs within one dB of signal-to-noise ratio (SNR) to the

Notation	Meaning
subscript k	time or packet index
$H_k \in \mathcal{S}_H$	channel amplitude
$R_k \in \mathcal{S}_R$	rate used for transmission
$\epsilon_k \in \{0, 1\}$	collision (1 if present, 0 if absent)
$A_k \in \{0, 1\}$	ACK (1 if PACK, 0 if NACK)
$\tilde{H}_k \triangleq \{H_k, \epsilon_k\}$	channel described by channel amplitude and collision
$C_k \in \mathcal{S}_C$	CSI
$\mathbf{r}_k, \mathbf{a}_k, \tilde{\mathbf{h}}_k$	vectors of rate, ACK and channel from time 0 to k (fixed long term statistics)
$\bar{\gamma}$	average SNR
$\bar{\rho}$	power correlation coefficient,
q_{ij}	collision transition probability $\epsilon = j$ to $\epsilon = i$
$t(R_k, H_k)$	throughput for packet k given rate and channel
$T(R_k; C_k)$	throughput for packet k given rate and CSI
π, π^*	policy, optimal policy (for rate adaptation)
$T(\pi), T^*$	throughput, optimal throughput
$b_k(\tilde{H}), \mathbf{b}_k$	belief state, collection of all belief states

TABLE I
KEY NOTATIONS USED IN THIS PAPER.

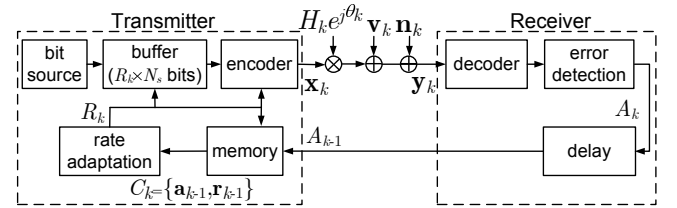


Fig. 1. System model for rate adaptation.

proposed upper bounds for a slowly changing channel, even in the presence of collisions.

Key notations are given in Table I. Section II describes the system model. Section III formulates the problem of maximizing the throughput averaged over an infinite horizon. To obtain a solution that approaches this throughput, Section IV considers the problem of maximizing the throughput averaged over a sliding window. Section V then solves this alternative problem using the PRA. Numerical results are presented in Section VI. Concluding remarks are given in Section VII.

II. SYSTEM MODEL

The system model is depicted in Fig. 1. The CSI available for rate adaptation at time k is denoted as C_k . This CSI consists of all past ACKs and all past rates, see Section II-C for further discussions. The time index k coincides with the packet index for simplicity. Based on C_k , the rate adaptation block selects a rate $R_k \in \mathcal{S}_R$, in bits per symbol, to transmit packet k . The rate determines the coding rate and modulation scheme used. The buffer collects $R_k N_s$ information bits from a source which are then encoded as a codeword $\mathbf{x}_k \in \mathbb{C}^{N_s}$, where N_s is the codeword length. Each codeword uses unit power per symbol on average. The codeword is finally sent as packet k . The bits are encoded and decoded independently for each packet, even in retransmissions. This ARQ scheme is commonly known as a Type I hybrid ARQ scheme [22].

We consider a flat-fading channel with (non-negative) channel amplitude $H_k \in \mathbb{R}_+$ that varies (slowly) between packets but is time invariant during each packet duration. Over a time

horizon of K packets, the received codeword is

$$\mathbf{y}_k = H_k e^{j\theta_k} \mathbf{x}_k + \mathbf{v}_k + \mathbf{n}_k, \quad k = 1, 2, \dots, K, \quad (1)$$

where $\mathbf{v}_k \in \mathbb{C}^{N_s}$ is multi-user interference and $\mathbf{n}_k \in \mathbb{C}^{N_s}$ is a circularly symmetric complex additive white Gaussian noise (AWGN) vector. The elements in \mathbf{n}_k are independent, each with zero mean and unit variance. We consider coherent detection by a receiver that knows and corrects the channel phase variations, so for simplicity we let $\theta_k = 0$. Without multi-user interference, the average SNR is given by $\bar{\gamma} = \mathbb{E}[H_k^2]$ for all k , assuming that H_k follows a stationary process.

The receiver performs decoding using \mathbf{y}_k with full knowledge of the channel state. Further, the rate is known, say via a packet header. Then, error detection is carried out for the packet, usually by using a cyclic redundancy check (CRC). The receiver sends an ACK bit A_k to the transmitter, either a PACK $A_k = 1$ for correct decoding, or a NACK $A_k = 0$ otherwise. Finally, the transmitter receives A_k with a packet delay, assumed to be received error-free.

Our subsequent analysis applies generally as long as the probabilities that relate the rates, ACKs and channels are well defined. For ease of obtaining numerical results, however, we make the following assumptions.

- A1: If multi-user interference is present at time k , i.e., $\mathbf{v}_k \neq \mathbf{0}$, then packet k is received with error. We say a *collision* has occurred, denoted as $\epsilon_k = 1$.
- A2: If multi-user interference is absent, i.e., $\mathbf{v}_k = \mathbf{0}$ or simply $\epsilon_k = 0$, then packet k is received correctly if and only if the rate R_k is below the AWGN channel capacity $C(H_k) = \log_2(1 + H_k^2)$.
- A3: Channel amplitudes and collisions occur independently, i.e., H_i is independent of ϵ_j for all i, j .

These assumptions are reasonable if multi-user interference is typically strong (for A1), a capacity-approaching coding scheme is employed (for A2), and all users transmit independently (for A3). Using assumptions A1, A2, the conditional PACK probability is given by

$$p(A_k = 1 | R_k, H_k, \epsilon_k) = \begin{cases} 1, & \epsilon_k = 0 \text{ and } R_k \leq C(H_k); \\ 0, & \text{otherwise.} \end{cases} \quad (2)$$

Here and subsequently, p denotes a probability mass function (pmf). The transmitter may thus infer from a PACK that no collision has occurred *and* R_k is low enough to support the transmission, or infer from a NACK that a collision has occurred *or* R_k is too high.

A. A Preview

To build intuition, let us preview the rate outputs of the particle-filter-based rate adaptation (PRA) to be proposed in Section V, based on assumptions A1, A2, A3. For clarity of presentation, a large, finely quantized set of rates S_R is available for rate adaptation.

In Fig. 2, there is no collision, i.e., the collision probability is zero. We see that generally the rate is adapted upwards if a PACK is received, and downwards if a NACK is received. The actual rate used depends on how much we can infer about the channel, by exploiting the available CSI. Instead, in Fig. 3, collision occurs with probability of 0.3. This relatively

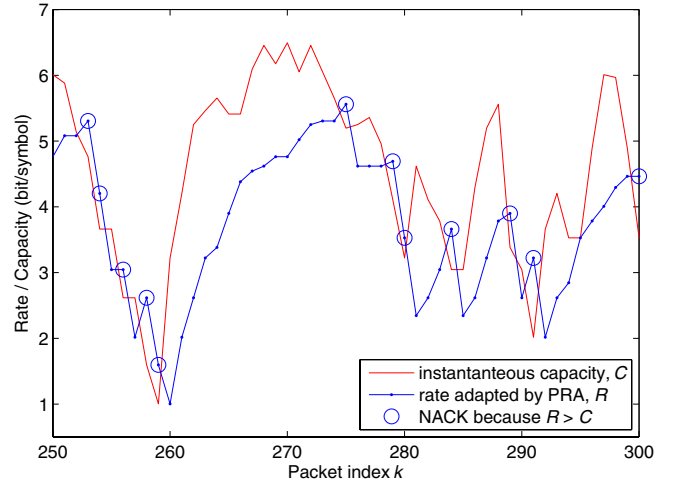


Fig. 2. Typical run of the rates adapted using PRA with ACK-rate CSI, zero probability of collision. Parameters: $\bar{\rho} = 0.95$, $\bar{\gamma} = 20$ dB, $q_{10} = 0$, $q_{01} = 1$.

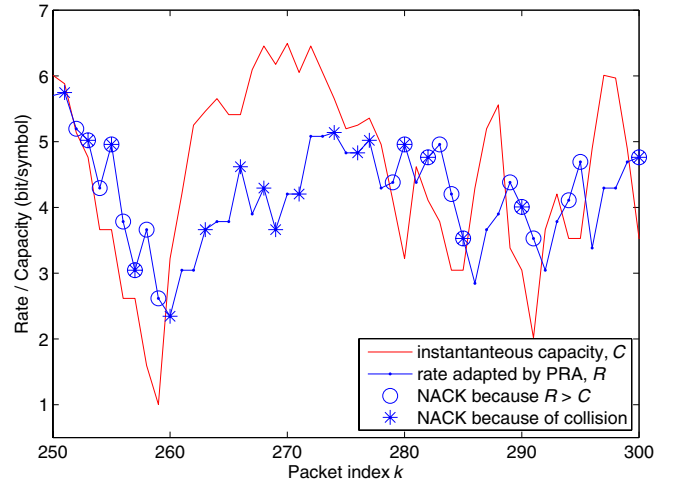


Fig. 3. Typical run of the rates adapted using PRA with ACK-rate CSI, 0.3 probability of collision. The instantaneous capacity is fixed to be the same as in Fig. 2, but here the transmitter cannot differentiate between the causes of the NACKs. Parameters: $\bar{\rho} = 0.95$, $\bar{\gamma} = 20$ dB, $q_{10} = 0.4$, $q_{01} = 0.9$.

high collision probability reflects a challenging scenario: it is ambiguous if a NACK occurs due to a channel fade or to a collision. To achieve high throughput, the PRA now takes collision into account and behaves differently compared to the case of no collision. For example, the rate may not necessarily be adapted downwards if a NACK is received, because the NACK may not be caused by a channel fade. In packets 250 – 260, a series of NACKs, even for packets transmitted at very low rates, suggests strongly that NACKs are caused primarily by collisions (which turns out to be partially true). Thus, it may even be worthwhile to *increase* the rate, which is done for packets 255 and 258, so that a high throughput is achieved if it turns out that no collision is present.

These examples suggest that throughput can be improved by exploiting all available information. Moreover, collision-aware rate adaptation policies can operate quite differently from collision-oblivious ones.

B. Channel Statistics

Except for the AWGN, the channel is completely described by the channel amplitude H_k and the collision event ϵ_k . Henceforth, we formally define the *channel* at time k as $\tilde{H}_k = \{H_k, \epsilon_k\}$, and the value that the channel takes as the *channel state*. For analytical tractability, we consider a first-order Markovian channel with distribution

$$p(\tilde{H}_k | \tilde{H}_0, \dots, \tilde{H}_{k-1}) = p(\tilde{H}_k | \tilde{H}_{k-1}) = p(H_k | H_{k-1})p(\epsilon_k | \epsilon_{k-1}), \quad (3)$$

for $H_k \in \mathcal{S}_H, \epsilon_k \in \{0, 1\}$, where the second equality follows from assumption A3. The subsequent analysis can be straightforwardly extended to an n th-order Markovian channel for $n \geq 2$, by defining the channel instead as $\tilde{H}_k = \{H_{k-n+1}, \dots, H_k, \epsilon_{k-n+1}, \dots, \epsilon_k\}$. Although an n th-order Markovian channel with larger n better approximates more realistic wireless channels, obtaining numerical results would incur significantly higher complexity (the size of the channel state space increases exponentially with n). We now give details on the statistics of H_k and ϵ_k for the FSMC characterized by (3).

1) *Channel Amplitude*: For our numerical results, we use the FSMC [20] to model temporal variations of H_k . We assume that H_k is in a discrete set $\mathcal{S}_H = \{h_1, \dots, h_N\}$ with N elements. First, we model the steady-state distribution $p(H_k)$ to be close to $f(G)$, where $f(G)$ is the probability density function (pdf) of the Rayleigh distribution, such that the approximation improves as N increases. To this end, we divide G 's support $(0, \infty)$ into N contiguous, non-overlapping parts. Let the n th part be bounded by (τ_{n-1}, τ_n) , where $\tau_0 = 0$ and $\tau_N \rightarrow \infty$. We choose $\{\tau_n\}$ such that the random variable G is in (τ_{n-1}, τ_n) with the same probability for all n , i.e., $\int_{\tau_{n-1}}^{\tau_n} f(G) dG = 1/N$ for all n . In [20], the n th state h_n is assigned as the mid-point of τ_{n-1} and τ_n , i.e., $h_n = (\tau_{n-1} + \tau_n)/2$. Instead, we assign $h_n = \tau_{n-1}$, which ensures that a PACK occurs only if $R_k \leq C(H_k = h_n)$. Next, we model the channel-amplitude transition probability $p(H_k | H_{k-1})$ such that $p(H_k = h_j | H_{k-1} = h_i) = \int_{\tau_{j-1}}^{\tau_j} \int_{\tau_{i-1}}^{\tau_i} f(G_k | G_{k-1}) dG_{k-1} dG_k$, where the bivariate Rayleigh distribution $f(G_k, G_{k-1})$ is fully determined by the power correlation coefficient [23, Eqn (1)]

$$\bar{\rho} = \text{cov}(G_k^2, G_{k-1}^2) / \sqrt{\text{var}(G_k^2) \text{var}(G_{k-1}^2)}. \quad (4)$$

Further details are found in [20]. The degree of the channel variations is reflected in $\bar{\rho}$: the closer it is to one, the slower the channel variation is. As an example, in Fig. 2 we set $\bar{\rho} = 0.95$, where the channel capacity varies as a result of channel fading. We see that the capacity becomes almost uncorrelated after a lag of more than around ten packets.

2) *Collision*: The collision transition probability is denoted as $q_{ij} \triangleq p(\epsilon_k = i | \epsilon_{k-1} = j)$. Since $\sum_i q_{ij} = 1$ and ϵ_k takes two possible values, the collision statistics can be completely specified by q_{10} and q_{01} . The steady-state collision probability can then be obtained as $p(\epsilon = 1) = q_{10}/(q_{01} + q_{10})$. In Fig. 3, for example, we have arbitrarily chosen $q_{01} = 0.4, q_{10} = 0.9$, so $p(\epsilon = 1) \approx 0.3$.

In our analysis, for simplicity we assume the parameters that describe the long-term channel statistics, namely $\bar{\gamma}, \bar{\rho}, q_{10}$

and q_{01} , to be known to the transmitter. In practice, these parameters may be tuned based on priori knowledge of the network or estimated online over a long time scale, see e.g. [24].

C. CSI

We initialize the ACK and rate as $A_0 = \emptyset, R_0 = \emptyset$, respectively, where \emptyset is the null value. The initial channel state $\tilde{H}_0 = \{H_0, \epsilon_0\}$ is randomly generated based on the steady-state distribution. We collect all ACKs until time k as vector $\mathbf{a}_k \triangleq [A_0, A_1, \dots, A_k]$, and similarly all rates, channel amplitudes and channel until time k as $\mathbf{r}_k, \mathbf{h}_k, \tilde{\mathbf{h}}_k$, respectively.

We study the maximum achievable throughput when the following CSI $C_k \in \mathcal{S}_C$ is available at the transmitter, while the receiver has full knowledge of the channel state for decoding. The CSI state space \mathcal{S}_C will be clear from the context. Define $C_0 = \emptyset$.

- *ACK-rate CSI*: $C_k = \{A_{k-1}, R_{k-1}, C_{k-1}\}$, or equivalently $C_k = \{\mathbf{a}_{k-1}, \mathbf{r}_{k-1}\}$. This CSI as depicted in Fig. 1 is the primary focus of our study. In words, the ACK-rate CSI consists of the most recent rate and ACK and also the past CSI, all available in a causal manner.
- *Full CSI*: $C_k = \tilde{H}_k$. The instantaneous channel \tilde{H}_k is provided as the CSI¹.
- *Delayed CSI*: $C_k = \tilde{H}_{k-1}$. Due to causality, full CSI cannot be provided in practice. Here, a delayed version of the channel (where the delay is one packet long) is provided as the CSI².
- *Periodic CSI*: In addition to the ACK-rate CSI, the transmitter is updated periodically with the delayed channel \tilde{H}_{k-1} , with period P . That is,

$$C_k = \begin{cases} \{\tilde{H}_{k-1}, A_{k-1}, R_{k-1}, C_{k-1}\}, & k \in \mathcal{S}_P, \\ \{A_{k-1}, R_{k-1}, C_{k-1}\}, & k \in \mathcal{S}_P^c, \end{cases} \quad (5)$$

where $\mathcal{S}_P = \{1, P+1, 2P+1, \dots\}$ and \mathcal{S}_P^c is its complementary set for positive indices.

- *No CSI*: $C_k = \emptyset$. No CSI is available (besides knowing the channel statistics).

We denote the maximum achievable throughput (to be precisely defined in Section III) corresponding to the above CSI as $T_{\text{ACK}}^*, T_{\text{full}}^*, T_{\text{delayed}}^*, T_{\text{periodic}}^*$ and T_{no}^* , respectively. We expect that with more extensive and more informative CSI, a larger maximum throughput can be achieved. Indeed, we will show in Section III that the maximum achievable throughputs can be ordered accordingly.

To describe the periodic CSI (5), it is sufficient to use a past channel \tilde{H}_τ and the truncated history of past ACKs and past rates from index τ onwards. Specifically, without loss of optimality in achieving T_{periodic}^* , the periodic CSI (5) can be reduced to (see Lemma 2 in Section III)

$$\hat{C}_k = \left\{ \tilde{H}_{\tau(k)}, [A_{\tau(k)+1}, \dots, A_{k-1}], [R_{\tau(k)+1}, \dots, R_{k-1}] \right\}. \quad (6)$$

¹The past CSI is not used to give $C_k = \{\tilde{H}_k, C_{k-1}\}$, as the channel is Markovian and so C_{k-1} does not contribute additional information on \tilde{H}_k .

²The past CSI is not used to give $C_k = \{\tilde{H}_{k-1}, C_{k-1}\}$, as the channel is Markovian and so C_{k-1} does not contribute additional information on \tilde{H}_{k-1} .

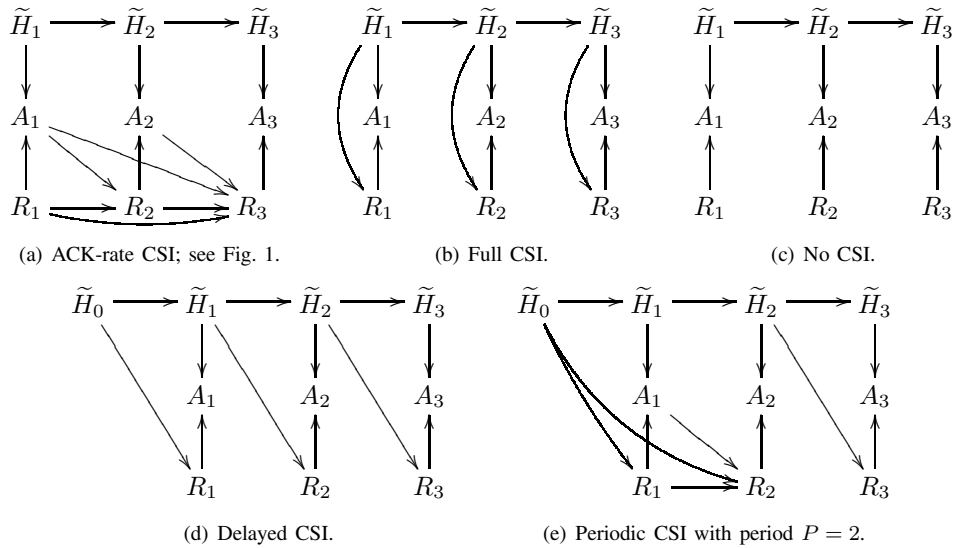


Fig. 4. Causal diagrams illustrating the dependence of channel \tilde{H}_k , ACK A_k and rate R_k as time progresses during rate adaptation. Different CSIs are available at the transmitter (a)-(e). In all cases, the channel is Markovian and the ACK depends on the rate and channel, while the rate depends on the CSI.

Here, $\tau(k) = P \lfloor (k-1)/P \rfloor$, where $\lfloor x \rfloor$ denotes the largest integer less than x . We interpret $\tau(k)$ as the most recent time index prior to k at which the channel is known exactly. Note that $\tilde{C}_k = \tilde{H}_{k-1}$ for $k \in \mathcal{S}_P$. To simplify analysis and implementation, we use the reduced form (6) over (5), unless otherwise stated.

D. Joint Distribution of Channels, Rates and ACKs

We treat the rate as a random variable, and the sequence of rates as a stochastic process over a time horizon of K packets. The causal relationship of the channel $\{\tilde{H}_k\}$, the ACKs $\{A_k\}$ and the rates $\{R_k\}$ can be represented with a directed graph [25], which can be established rigorously as a *causal diagram* [26]. Let X_k be a random variable at time k and let \mathcal{A}_k be the set of all random variables at time k or earlier *except* X_k . If $p(X_k|\mathcal{A}_k) = p(x_k|\mathcal{B}_k)$ where \mathcal{B}_k is the smallest possible subset of \mathcal{A}_k , then we draw an arrow from each of the random variables in \mathcal{B}_k to X_k . Intuitively we may say that the random variable X_k is *caused* only by the random variables in \mathcal{B}_k .

Besides providing a graphical overview of how the random variables interact, a causal diagram allows any conditional independence to be easily established [25], [26]. The causal diagrams for different CSIs are illustrated in Fig. 4 for $K = 3$, based on the following considerations. For all k , we have $\tilde{H}_k \rightarrow \tilde{H}_{k+1}$ since the channel is Markovian. Moreover, the probability of a PACK or NACK depends only on the present channel and rate, thus we have $\{\tilde{H}_k, R_k\} \rightarrow A_k$. Finally, we let each rate depend only on its corresponding CSI, so that $C_k \rightarrow R_k$. For any CSI, the joint pmf of $\tilde{\mathbf{h}}_K, \mathbf{a}_K, \mathbf{r}_K$ can then be factored as

$$p(\tilde{\mathbf{h}}_K, \mathbf{a}_K, \mathbf{r}_K) = \prod_{k=1}^K p(\tilde{H}_k|\tilde{H}_{k-1})p(R_k|C_k)p(A_k|R_k, \tilde{H}_k). \quad (7)$$

E. Rate Adaptation

Rate adaptation is performed through a *policy* π , defined by the set of $p(R_k|C_k)$ for all k and all C_k . In practice

typically a (deterministic) function f_k selects the rate to be used at time k , i.e., $R_k = f_k(C_k)$. In this case, the policy is *deterministic*. Then in (7), we can substitute for $p(R_k|C_k)$ the Kronecker delta function $\delta(R_k - f_k(C_k))$. Moreover, if $f_k(C_k)$ is independent of k for all C_k , we say that the policy π is *stationary*. Strictly speaking, many types of CSI, like the ACK-rate CSI, do not admit a stationary policy. This is because the size of the CSI grows as time progresses, which necessitates a different f_k (with input of different length) for different k . However, we will show that each CSI can be equivalently mapped into the belief state, which has the same dimension for any k . Thus, a policy for different types of CSI when defined over the belief states can still be stationary.

F. Throughput

If packet k is received correctly, it contributes an *instantaneous throughput* given by the data rate R_k . This occurs when $A_k = 1$. If $A_k = 0$, the packet is lost in an outage and it is discarded (a common practice in delay-sensitive applications) or retransmitted. In both cases the instantaneous throughput is zero. Given the channel state \tilde{H}_k , the expected throughput for packet k encoded at rate R_k is thus

$$t(R_k, \tilde{H}_k) = R_k p(A_k = 1 | R_k, \tilde{H}_k). \quad (8)$$

If the channel is not known exactly, the expected throughput for packet k given CSI C_k is then

$$\begin{aligned} T(R_k; C_k) &= \mathbb{E}_{\tilde{H}_k|C_k} [t(R_k, \tilde{H}_k)] \\ &= \sum_{\tilde{H}_k} p(\tilde{H}_k|C_k) t(R_k, \tilde{H}_k). \end{aligned} \quad (9)$$

Here, the expectation is performed over the *a posteriori* channel pmf $p(\tilde{H}_k|C_k)$, which we denote as

$$b_k(\tilde{H}_k) = p(\tilde{H}_k|C_k) \quad (10)$$

for a given CSI C_k . We call b_k the *belief state*. Given C_k , the set of all belief states $\mathbf{b}_k \triangleq \{b_k(\tilde{H}) \forall \tilde{H}\}$ is sufficient

to compute the expected throughput. Using (2), (8) and assumption A3, (9) becomes

$$T(R_k; C_k) = R_k \Pr(R_k < C(H_k)|C_k) p(\epsilon_k = 0|C_k). \quad (11)$$

III. MAXIMIZING INFINITE-HORIZON THROUGHPUT

In this section, we consider the maximization of the throughput over an infinite time horizon. We derive expressions for the maximum achievable throughput for different types of CSI, and a sequence of inequalities that relate them. In addition, we derive two upper bounds on the throughput achieved with ACK-rate CSI, both of which are tighter than previously known bounds.

A. Problem Formulation

For any type of CSI, the *long-term throughput* $\mathcal{T}(\pi)$ given policy π is obtained by averaging the expected throughput over an infinite-time horizon, i.e.,

$$\mathcal{T}(\pi) = \lim_{K \rightarrow \infty} \frac{1}{K} \mathbb{E} \left[\sum_{k=1}^K T(R_k; C_k) \right]. \quad (12)$$

The expectation is defined with respect to the joint pmf (7).

Using the ACK-rate CSI $C_k = \{\mathbf{a}_{k-1}, \mathbf{r}_{k-1}\}$, the *maximum achievable throughput* obtained by the optimal rate adaptation policy π^* is denoted by

$$\mathcal{T}_{\text{ACK}}^* = \max_{\pi} \mathcal{T}(\pi) = \mathcal{T}(\pi^*). \quad (13)$$

In general, the superscript $*$ denotes optimality while the subscript denotes the type of CSI used.

Our objective is to find a rate adaptation policy using the ACK-rate CSI that achieves a throughput close to $\mathcal{T}_{\text{ACK}}^*$. In addition we wish to obtain tight upper bounds for $\mathcal{T}_{\text{ACK}}^*$ that can be practically computed.

B. Main Analytical Results and Discussions

The maximum achievable throughput $\mathcal{T}_{\text{ACK}}^*$ for ACK-rate CSI is given by maximizing (12). Similarly, the maximum achievable throughput $\mathcal{T}_{\text{full}}^*$ for full CSI, $\mathcal{T}_{\text{delayed}}^*$ for delayed CSI, $\mathcal{T}_{\text{periodic}}^*$ for periodic CSI and $\mathcal{T}_{\text{no}}^*$ for no CSI are defined by maximizing (12) with the corresponding C_k .

Theorem 1 states the analytical expressions for $\mathcal{T}_{\text{full}}^*$, $\mathcal{T}_{\text{delayed}}^*$, $\mathcal{T}_{\text{periodic}}^*$ and $\mathcal{T}_{\text{no}}^*$.

A policy is said to be *myopic* if for every packet, the rate is adapted to maximize only the current expected throughput, without concerns about the effect on future achievable throughput. The throughput achieved by a myopic policy with CSI C_k is thus $\mathbb{E}_{C_k} [\max_{R_k} T(R_k; C_k)]$.

Theorem 1: The maximum achievable throughput for full CSI, delayed CSI or no CSI is achieved by a stationary myopic

policy, which can be expressed respectively as

$$\mathcal{T}_{\text{full}}^* = \mathbb{E}_{\tilde{H}_k} \left[\max_{R_k} T(R_k; \tilde{H}_k) \right] \quad (14a)$$

$$= q_0 \mathbb{E}_{H_k} \left[\max_{R_k} T(R_k; H_k, \epsilon = 0) \right] \quad (14b)$$

$$\mathcal{T}_{\text{delayed}}^* = \mathbb{E}_{\tilde{H}_{k-1}} \left[\max_{R_k} T(R_k; \tilde{H}_{k-1}) \right] \quad (15a)$$

$$= q_0 \mathbb{E}_{H_{k-1}} \left[\max_{R_k} R_k \Pr(R_k < C(H_k)|H_{k-1}) \right] \quad (15b)$$

$$\mathcal{T}_{\text{no}}^* = \max_{R_k} T(R_k; \emptyset) \quad (16a)$$

$$= q_0 \max_{R_k} R_k \Pr(R_k < C(H_k)) \quad (16b)$$

where we denote $q_0 = p(\epsilon = 0)$. The maximum achievable throughput for periodic CSI with period P is given by

$$\mathcal{T}_{\text{periodic}}^* = \mathbb{E}_{C_1} [J_1(C_1)] / P, \quad (17)$$

where J_1 can be expressed recursively with decreasing $k = P, P-1, \dots, 1$ according to

$$J_k(C_k) = \max_{R_k} T(R_k; C_k), \quad k = P \quad (18a)$$

$$J_k(C_k) = \max_{R_k} \{T(R_k; C_k) + \mathbb{E}_{C_{k+1}|C_k} [J_{k+1}(C_{k+1})]\}, \quad k = P-1, \dots, 1. \quad (18b)$$

Proof: We employ Bellman's equations [27] for our proof; see Section III-C for details. ■

Theorem 2 orders the maximum achievable throughput for different CSI.

$$\textit{Theorem 2: } \mathcal{T}_{\text{full}}^* \geq \mathcal{T}_{\text{delayed}}^* \geq \mathcal{T}_{\text{periodic}}^* \geq \mathcal{T}_{\text{ACK}}^* \geq \mathcal{T}_{\text{no}}^*.$$

Proof: We rely on (7) implicitly and on Theorem 1; see Appendix B for details. ■

From Theorem 2, we see that $\mathcal{T}_{\text{periodic}}^*$ is an upper bound of $\mathcal{T}_{\text{ACK}}^*$. Moreover, $\mathcal{T}_{\text{periodic}}^*$ is at least as tight as $\mathcal{T}_{\text{delayed}}^*$. In [18], $\mathcal{T}_{\text{delayed}}^*$ has been used as an upper bound for $\mathcal{T}_{\text{ACK}}^*$.

Theorem 3 introduces another upper bound given by

$$\mathcal{T}_{\text{ub}} = \mathbb{E}_{\tilde{H}_{k-2}} \left[\max_{R_{k-1}} \mathbb{E}_{R_{k-1}, A_{k-1} | \tilde{H}_{k-2}} \left[\max_{R_k} T(R_k; \bar{C}_k) \right] \right], \quad (19)$$

where $\bar{C}_k \triangleq \{R_{k-1}, A_{k-1}, \tilde{H}_{k-2}\}$.

$$\textit{Theorem 3: } \mathcal{T}_{\text{delayed}}^* \geq \mathcal{T}_{\text{ub}} \geq \mathcal{T}_{\text{ACK}}^*.$$

Proof: See Appendix C for a proof. ■

This new upper bound \mathcal{T}_{ub} is at least as tight as $\mathcal{T}_{\text{delayed}}^*$. The superscript $*$ is omitted in this notation \mathcal{T}_{ub} , because the policy that achieves \mathcal{T}_{ub} is genie-aided and cannot be implemented in practice. From numerical simulations in Section VI, \mathcal{T}_{ub} can be even tighter than $\mathcal{T}_{\text{periodic}}^*$.

We interpret (19) as a maximization of the throughput $T(R_k; \bar{C}_k)$ at time k with CSI \bar{C}_k . This CSI consists of the past rate, past ACK and a channel amplitude delayed by *two* units of time. We note that the past rate R_{k-1} had been optimized given CSI \tilde{H}_{k-2} which is relatively delayed by *one* unit of time.

Intuitively, two aspects make \mathcal{T}_{ub} achieve a higher throughput than $\mathcal{T}_{\text{ACK}}^*$. Firstly, the CSI \bar{C}_k available for adapting R_k is more informative than in the case of ACK-Rate CSI, with \tilde{H}_{k-2} being the additional CSI. Secondly, both past and current rates are used to maximize the current throughput (for

packet k), without regarding how past throughput (for packet $k - 1$) and future throughput (for packet $k + 1$ onwards) are affected. Since past and present rates are *always* used to optimize for the current packet, this policy is genie-aided and cannot be implemented over an infinite time horizon.

We can generalize T_{ub} . For a delay-related parameter $D \geq 1$, we make the common CSI \tilde{H}_{k-D} available to all D packets, namely packet $k - D + 1$ to packet k , in addition to their ACK-rate CSI. We then concurrently adapt the rates for these packets to maximize the throughput of packet k . Clearly, $D = 1$ corresponds to the case of delayed CSI, while $D = 2$ corresponds to (19).

C. Expressions for the Maximum Achievable Throughput

We now prove Theorem 1. We refer to the value that a CSI takes as a CSI state. Lemma 1 states an important result from optimal control that is useful for subsequent derivations.

Lemma 1: Suppose that for all initial CSI states and all policies, there exists at least one CSI state in its state space \mathcal{S}_C that is visited at least once with positive probability within some bounded time. Then, the maximum achievable throughput T^* obtained by maximizing (12) satisfies Bellman's equation

$$T^* + \nu(C) = \max_R \left\{ T(R; C) + \sum_{C' \in \mathcal{S}_C} p(C'|C, R) \nu(C') \right\} \quad (20)$$

for all CSI states C in \mathcal{S}_C . Here, $\nu(C)$ is an auxiliary function known as the differential reward function³ and $p(C'|C, R)$ is the transition probability from state C to state C' given rate R . Moreover, a policy where the rate R satisfies (20) for all CSI states C in \mathcal{S}_C is optimal, i.e., this stationary policy achieves T^* .

Proof: See Section 7.4 of [27], rephrased for our throughput maximization problem. ■

To prove Theorem 1, we assume that $q_{01} > 0$ and $q_{10} > 0$, hence collision occurs with non-zero probability. The case of $q_{01} = q_{10} = 0$ where collision never occur⁴ can be proved similarly, if we let $\epsilon = 0$ and define the channel to consist only of the channel amplitude, i.e., $\tilde{H} = \{H\}$.

1) *Full CSI:* For full CSI, the CSI state space is $\mathcal{S}_C = \mathcal{S}_H \times \{0, 1\}$, where \mathcal{S}_H is the channel state space and $\{0, 1\}$ is the collision state space. Since any CSI state transits to another CSI state with a positive probability for any policy, Lemma 1 applies. By letting $C = \tilde{H}_k$ and $C' = \tilde{H}_{k+1}$, we have $p(C'|C, R) = p(C'|C)$ because \tilde{H}_k is Markovian, thus Bellman's equation becomes

$$T^* + \nu(C) = \max_R T(R; C) + \sum_{C' \in \mathcal{S}_C} p(C'|C) \nu(C'). \quad (21)$$

This maximization needs only to be performed for the function T , independent of the differential reward function ν . This shows that a (stationary) myopic policy achieves the maximum throughput in (21) and is thus optimal according to Lemma 1.

³Typically the differential reward function has to be solved jointly with T^* using Bellman's equation, so as to obtain T^* .

⁴The case when collision occurs with probability one is clearly not interesting.

Hence, the maximum achievable throughput is given by (14a), while (14b) is obtained using (11).

From the above derivations, the myopic policy is optimal for any CSI type if $p(C'|C, R_k) = p(C'|C)$ for all C . This means that the rate R_k will not affect the future CSI state C' nor the future throughput (which depends on C'), thus intuitively we can focus on maximizing only the current throughput.

2) *Delayed CSI:* For delayed CSI, the CSI state space is the same as for full CSI, so Lemma 1 applies. In this case, we let $C = H_{k-1}$ and $C' = H_k$. Similarly $p(C'|C, R_k) = p(C'|C)$ for all C , so the myopic policy is again optimal. Hence, we obtain (15a), while (15b) is obtained using (11).

3) *No CSI:* For no CSI, the CSI state space consists of only the null value \emptyset . Hence, we have $p(C'|C, R_k) = p(C'|C)$ trivially and so the myopic policy is optimal. Thus, we use a fixed rate to maximize $\mathbb{E}_H[T(R; \emptyset)]$ for all packets. Hence, we obtain (16a), while (16b) is obtained using (11).

4) *Periodic CSI:* For periodic CSI (and also ACK-rate CSI), the myopic policy is generally sub-optimal. Lemma 2, however, allows us to simplify analysis by using the reduced periodic CSI (6), instead of the original periodic CSI (5).

Lemma 2: The maximum achievable throughput for periodic CSI (5) is the same as the maximum achievable throughput for the reduced CSI (6).

Proof: For clarity, let us denote, at time k , the periodic CSI as \tilde{C}_k and the reduced CSI as \hat{C}_k . To show that the maximum achievable throughput is the same for both CSIs, it is sufficient to show that the belief state $b_k = p(\tilde{H}_k | C_k)$ is the same for both CSIs $C_k = \tilde{C}_k$ and $C_k = \hat{C}_k$ for all k . This is because the belief state serves as a sufficient input for a policy to determine the next rate (whether the policy is optimal or not).

Using the relationships $\tilde{H}_k \rightarrow \tilde{H}_{k+1}$ and $\{\tilde{H}_k, R_k\} \rightarrow A_k$, from (5) we can write

$$\begin{aligned} & p(\tilde{H}_k | C_k = \tilde{C}_k) \\ &= \begin{cases} p(\tilde{H}_k | \tilde{H}_{k-1}), & k \in \mathcal{S}_P; \\ \sum_{\tilde{H}_{k-1}} p(\tilde{H}_{k-1} | C_k = \hat{C}_k) p(\tilde{H}_k | \tilde{H}_{k-1}), & k \in \mathcal{S}_P^c, \end{cases} \quad (22) \end{aligned}$$

where \hat{C}_k is given by (6) for $k \in \mathcal{S}_P^c$. Moreover, it can be verified that $p(\tilde{H}_k | C_k = \hat{C}_k)$ is also given by the right-hand side of (22). Since the belief state given \tilde{C}_k and given \hat{C}_k is equivalent, the maximum achievable throughput is the same for both periodic and reduced CSIs. ■

From the reduced CSI (6), Lemma 2 shows that past CSI prior to $\tau(k)$ can be discarded. This result is intuitively reasonable: since the channel is modeled as Markovian, the knowledge of an exact channel amplitude makes priori CSI redundant. However, the subsequent CSI after $\tau(k)$, when the channel amplitude is not yet exactly known, still needs to be retained. We can thus consider the policy over a single period of P packets. The first packet in this period receives a CSI consisting of an independent realization of the delayed channel amplitude, while the remaining packets receive an ACK-rate CSI. The throughput over an infinite-time horizon is then equal to the throughput averaged over this period, i.e.,

$$T_{\text{periodic}}(\pi) = \frac{1}{P} \mathbb{E} \left[\sum_{k=1}^P T(R_k; \hat{C}_k) \right], \quad (23)$$

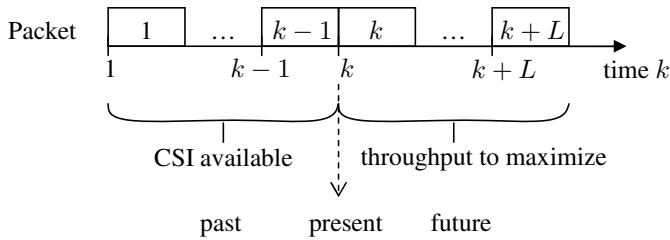


Fig. 5. Using CSI from the past to maximize throughput in the future.

where \hat{C}_k is given by (6). Here, we assume that a periodic policy is used. That is, the rate is adapted in the same way for all packets spaced apart by period P . An optimal policy, if it exists, is also given by a periodic policy. This is because if we have a non-periodic optimal policy, we can choose to repeat the policy over the particular period that maximizes the throughput (23); this new periodic policy gives the same throughput, or higher. This justifies us to focus on one period of a periodic policy.

Let $J_k, k = 1, \dots, P$, be the maximum throughput accumulated over packet k to packet P , given CSI state C_k at time k . The maximum achievable throughput (23) can then be obtained from Bellman's equation *with finite time horizon* [27], given by

$$T_{\text{periodic}}^* = \max_{\pi} T_{\text{periodic}}(\pi) = \mathbb{E}_{C_1} [J_1(C_1)] / P \quad (24)$$

where J_k is computed using (18). To obtain $J_1(C_1)$ and hence T_{periodic}^* , we can perform a backward recursion. This is done by first obtaining (18b) for all possible CSI C_P , then obtaining (18c) for all possible $C_k, k = P-1, \dots, 1$. The overall complexity is dominated by the first recursion, whose complexity increases exponentially with P . However, computation is still feasible for small P .

IV. MAXIMIZING SLIDING-HORIZON THROUGHPUT

To find the optimal policy π^* with ACK-rate CSI is a PSPACE-complete problem even if the horizon is finite [19]. A PSPACE-complete problem is solved using a polynomial amount of memory and unlimited time and is considered at least as hard as an NP-complete problem. To obtain an implementable policy that achieves close to the maximum achievable throughput T_{ACK}^* , this section solves an alternative problem by considering a finite time horizon. Although the solution for this alternative problem still cannot be implemented exactly, it allows a highly accurate approximate solution to be realized via a particle filter, which will be considered in Section V.

A. Problem Formulation with Sliding Window

For FSMC, the autocorrelation function of the channel amplitude appears to decrease exponentially with increasing time lag [20]. Hence, the validity of the information provided by the CSI diminishes rapidly into the future. As such, there may be little loss if a policy maximizes average throughput over a *finite horizon*, even though in the original problem the horizon is infinite.

We thus consider an alternative problem by limiting the horizon, see Fig. 5. At time k (the present), we are given the ACK-rate CSI C_k (from the past). We wish to maximize the (future) throughput of next $L+1$ packets given by

$$T_{\text{SH}}(\pi_k; C_k) = \frac{1}{L+1} \mathbb{E} \left[\sum_{l=k}^{k+L} T_l(R_l; C_l) \right] \quad (25)$$

by varying the policy π_k consisting of rates of packets $k, \dots, k+L$. We call T_{SH} the *sliding-horizon throughput* since as time k progresses, the time horizon shifts forward. From the optimum policy π_k , we then use the optimum rate R_k^o corresponding to packet k for transmission, i.e.,

$$R_k^o = \arg \max_{R_k} \left\{ \max_{\pi_k \setminus R_k} T_{\text{SH}}(\pi_k; C_k) \right\} \quad (26)$$

where $\pi_k \setminus R_k$ refers to the rates in policy π_k except for R_k . Thus, we may treat the future rates as auxiliary variables which are tentatively optimized but may be discarded once R_k^o is obtained. Next, at time $k+1$, the ACK A_{k+1} is received and the CSI C_{k+1} is updated. The process of obtaining R_k^o based on (25), (26) with k replaced by $k+1$ is then performed, and so on for subsequent packets as the next ACK is received.

In (25), L is taken as a fixed parameter. As L increases, the effects of rate adaptation on future throughput are better taken into account so the corresponding throughput is expected to improve. When L approaches infinity, R_k maximizes the throughput averaged over an infinite-time horizon and hence achieves the maximum throughput T^* . In the remainder of this paper, we consider $L = 0, 1$. Extensions for larger L can be carried out similarly but with an exponential increase in the complexity of optimization.

B. Myopic Optimization: $L = 0$

We defer the implementation details for $L = 1$ to the next section. For $L = 0$, we do not need to consider how future throughput is affected. Thus, equivalently we use a myopic policy according to $R_k = \arg \max_{R_k} \mathbb{E} [T(R_k; C_k)]$. This policy is also equivalent to the Q-MDP policy considered in [18], as shown next.

The Q-MDP policy is based on a general heuristic strategy first proposed in [28]. This policy solves another alternative problem, in which ACK-rate CSI is available for the present packet but full CSI is assumed to be available in the next immediate packet. That is, $C_k = [\mathbf{a}_{k-1}, \mathbf{r}_{k-1}]$ is given at time k while $C_{k+1} = \hat{H}_{k+1}$ (not yet known at time k) will be given at time $k+1$. The rate R_k is then chosen to maximize the throughput of packet $k, k+1, \dots$. We note that R_k cannot affect the future CSI $C_i, i \geq k+1$, given that the channel is known exactly, nor affect the future instantaneous throughput of packet i . Thus, the Q-MDP policy reduces to the myopic policy where only the throughput of packet k is maximized. This conclusion holds in this paper where the bit buffer is never empty. In [18] where the buffer can be empty, however, the Q-MDP and the myopic policies can be different. This is because the CSI state includes the (limited) buffer queue length, and hence the future CSI and throughput can be affected by R_k .

V. PARTICLE-FILTER-BASED RATE ADAPTATION (PRA)

This section shows that the implementation of maximizing the sliding-horizon throughput for ACK-rate CSI is mainly determined by how the belief states are stored and maintained over time. To reduce the high implementation complexity, we propose using the particle filter. Before we introduce the particle filter in Section V-B, we first analyze the bottlenecks in directly computing the sliding-window throughput.

A. Direct Computation

Consider $L = 0$. The optimal policy is obtained by maximizing the throughput $T(R_k; C_k)$, which can be straightforwardly computed given the belief states.

Consider $L = 1$. The policy π_k consists of the rate R_k for the current packet and also of *both* rates $R_{k+1}(A_k = 0), R_{k+1}(A_k = 1)$ for the next packet, depending on the yet-to-be-known ACK A_k . We can express (25) as

$$\begin{aligned} & 2T_{\text{SH}}(\pi_k; C_k) \\ &= T_k(R_k; C_k) + \mathbb{E}_{A_k|C_k, \pi_k} [T_{k+1}(R_{k+1}(A_k); C_{k+1})] \quad (27) \\ &= T_k(R_k; C_k) + \mathbb{E}_{\tilde{H}_k, A_k|C_k, \pi_k} [T_{k+1}(R_{k+1}(A_k); C_{k+1})] \quad (28) \\ &= T_k(R_k; C_k) \\ &+ \mathbb{E}_{\tilde{H}_k|C_k} \mathbb{E}_{A_k|\tilde{H}_k, R_k} [T_{k+1}(R_{k+1}(A_k); C_{k+1})]. \quad (29) \end{aligned}$$

Here, (27) follows since A_k is the remaining random variable in (25) given C_k, π_k , (28) follows from introducing the channel \tilde{H} which is a hidden random variable and (29) follows from the joint pmf (7).

The two terms in (29) are the expected throughput of packet $k, k+1$, respectively, given CSI C_k and policy π_k . We write (29) in terms of the belief states $\{b_{k+1}(H_k)\}$ corresponding to the CSI C_k , and the belief states $\{b_{k+1}(\tilde{H}_{k+1}, A_k, R_k)\}$ corresponding to the future CSI $C_{k+1} = [A_k, R_k, C_k]$, to give

$$\begin{aligned} & 2T_{\text{SH}}(\pi_k; C_k) \\ &= \sum_{\tilde{H}_k} b_k \left[t_k(R_k; C_k) \right. \\ &+ \left. \mathbb{E}_{A_k|\tilde{H}_k, R_k} \left[\sum_{\tilde{H}_{k+1}} b_{k+1}(A_k) t_{k+1}(R_{k+1}(A_k); C_{k+1}) \right] \right] \quad (30) \\ &+ \mathbb{E}_{A_k|\tilde{H}_k, R_k} \left[\sum_{\tilde{H}_{k+1}} b_{k+1}(A_k) t_{k+1}(R_{k+1}(A_k); C_{k+1}) \right] \quad (31) \end{aligned}$$

by using (9). For brevity we subsequently omit the arguments in $b_k(\tilde{H}_k), b_{k+1}(\tilde{H}_{k+1}, A_k, R_k)$. Note that t_k can be obtained using (8). To compute the throughput (31), what remain to obtain are the belief states.

1) *Maintaining the Belief States:* The Markov property of the channel allows the belief state b_k to be obtained recursively by using the *prediction* and *update* steps given by

$$\begin{aligned} b_k &= p(\tilde{H}_k|C_k) = \sum_{\tilde{H}_{k-1}} p(\tilde{H}_k|\tilde{H}_{k-1})p(\tilde{H}_{k-1}|C_k), \quad (32) \\ p(\tilde{H}_{k-1}|C_k) &\propto p(\tilde{H}_{k-1}|\mathbf{a}_{k-2}, \mathbf{r}_{k-1}) \\ &\quad \times p(A_{k-1}|\tilde{H}_{k-1}, \mathbf{a}_{k-2}, \mathbf{r}_{k-1}) \\ &= b_{k-1} p(A_{k-1}|\tilde{H}_{k-1}, R_{k-1}), \quad (33) \end{aligned}$$

respectively. The last line of the update step results from (7), or by exploiting the conditional independence in Fig. 4(a).

Recall that \mathbf{b}_k is the set of the belief states over all \tilde{H}_k . To compute a specific belief state b_k in \mathbf{b}_k , clearly from (32),

(33) we need to only maintain in memory $\mathbf{b}_{k-1}, R_{k-1}, A_{k-1}$. Consequently, without any loss of information, we can discard all past beliefs $\mathbf{b}_1, \dots, \mathbf{b}_{k-2}$ and all past CSIs except for R_{k-1}, A_{k-1} . We note that \mathbf{b}_{k+1} , which is used to predict the channel at time $k+1$ in (31), can also be computed using \mathbf{b}_k for a given (tentative) rate R_k and ACK A_k .

2) *Issues with Maintaining Belief States:* There are two advantages of maintaining the most current belief states and ACK-rate CSI, instead of all ACK-rate CSIs. First, the belief states allow direct computation of the throughput. Second, the space of the belief state is fixed, while the space of the CSI grows as time progresses. However, the disadvantage is that the computation in the prediction step is complex if the number of channel states N is large. Moreover, it is impossible to keep the belief state in memory accurately, as \mathbf{b}_k lies in a (real) probability space of dimension $N-1$. To solve these problems, we consider an approximate but highly accurate technique based on a sequential Monte Carlo method, known as the particle filter [29].

B. Proposed Computation via Particle Filter

We employ the particle filter to maintain the belief states and to estimate the throughput. The particle filter is a sequential Monte Carlo method that estimates a pmf or pdf by a recursive importance sampling of random samples, known as particles. Particle filters are popularized by the sampling importance resampling (SIR) filter in [21].

At time k , the particle filter maintains in memory the random measure $\chi_k = \left\{ \left(\tilde{H}_k^{(n)}, w_k^{(n)} \right), n = 1, \dots, N_p \right\}$, where $\tilde{H}_k^{(n)}$ is the n th particle with weight $w_k^{(n)}$. For initialization, we may independently generate $\tilde{H}_0^{(n)}$ according to the probability $p(\tilde{H})$ and fix $w_0^{(n)} = 1/N_p$ for all n . The random measure χ_k forms an estimate of the belief states at time k according to

$$b_k \approx \sum_{n=1}^{N_p} w_k^{(n)} \delta(\tilde{H}_k - \tilde{H}_k^{(n)}). \quad (34)$$

The random measure χ_k is generated recursively over time via Monte Carlo sampling [21], based on the knowledge of the system dynamics (governed by the probabilities $p(\tilde{H}_k|\tilde{H}_{k-1}), p(A_{k-1}|\tilde{H}_{k-1}, R_{k-1})$), and on the latest observed acknowledgement and rate. Specifically, given $\tilde{H}_{k-1}^{(n)}$, we independently generate $\tilde{H}_k^{(n)}$ with the importance sampling function $p(\tilde{H}_k|\tilde{H}_{k-1} = \tilde{H}_{k-1}^{(n)})$. Then, given $w_{k-1}^{(n)}$, we assign the weight of the n th particle as $w_k^{(n)} = w_{k-1}^{(n)} p(A_{k-1}|\tilde{H}_{k-1} = \tilde{H}_{k-1}^{(n)}, R_{k-1})$. Finally, normalization is carried out so that all weights in time k sum to unity. From χ_{k-1} we can thus obtain χ_k . Similarly, from χ_k we can obtain χ_{k+1} given (tentative) A_k, R_k . Then, χ_{k+1} is used to approximate the belief state at time $k+1$ as

$$b_{k+1}(A_k, R_k) \approx \sum_{m=1}^{N_p} w_{k+1}^{(m)}(A_k, R_k) \delta(\tilde{H}_{k+1} - \tilde{H}_{k+1}^{(m)}). \quad (35)$$

Finally, substituting (8), (34) and (35) into (31) allows the throughput to be approximated as

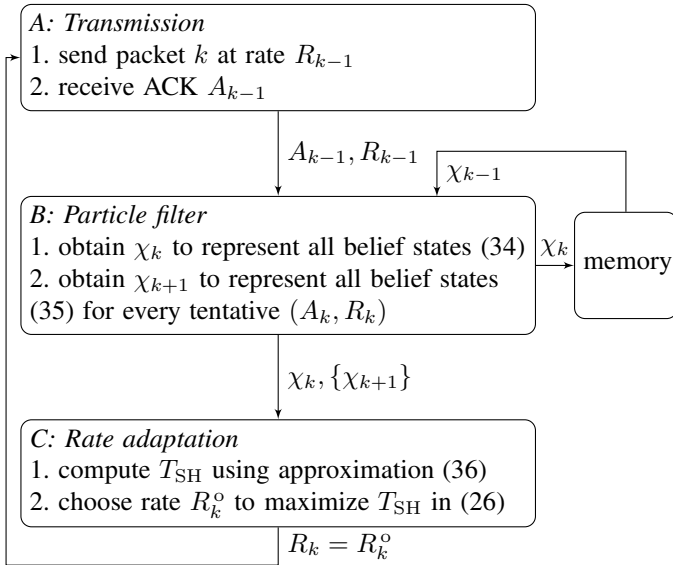


Fig. 6. Summary of implementation of PRA for $L = 1$.

$$\begin{aligned}
 2T_{\text{SH}}(\pi_k; C_k) &\approx \sum_{n=1}^{N_p} w_k^{(n)} \left(p(A_k = 1 | R_k, \tilde{H}_k = \tilde{H}_k^{(n)}) \right. \\
 &\left. + \mathbb{E}_{A_k | \tilde{H}_k, R_k} \left[\sum_{m=1}^{N_p} w_{k+1}^{(m)}(A_k) p(A_k = 1 | R_k, \tilde{H}_k = \tilde{H}_k^{(m)}) \right] \right). \quad (36)
 \end{aligned}$$

This approximation improves as the total number of particles N_p is increased.

Fig. 6 highlights the key steps to implement the PRA for rate adaptation. Although we are initially given the ACK-rate CSI $C_k = \{A_{k-1}, R_{k-1}, C_{k-1}\}$, we see from Fig. 6 that $\{A_{k-1}, R_{k-1}, \chi_k\}$ is used as input to the particle filter. As $N_p \rightarrow \infty$, this input becomes sufficient for throughput maximization (as the approximation (36) becomes accurate) and may then be treated to be equivalent to the ACK-rate CSI.

Particle filters may experience the degeneracy phenomenon [29], where all but one particle will have negligible weight after several recursions. Solutions to circumvent this problem are described in [29]. We follow [21] by resampling the particles, which effectively normalizes the weights uniformly after every recursion. In our simulations, we did not see the degeneracy phenomenon over runs of 1000 packets.

VI. NUMERICAL STUDY

For our numerical studies, we discretize the channel amplitude $H \in \mathcal{S}_H$ by using $N = 100$ channel states, as described in Section II-B. To reduce the effects of rate quantization and to observe the full dynamic behavior of rate adaptation, we match the set of available rates \mathcal{S}_R to the channel state space, according to $\mathcal{S}_R = \{C(H), H \in \mathcal{S}_H\}$. To give accurate results we use $N_p = 1000$ particles.

Typical runs of the PRA, without and with collisions, have been shown in Figs. 2–3, respectively. The channel amplitudes (same in both figures) are generated randomly at an average SNR of $\bar{\gamma} = 20$ dB and a power correlation coefficient of $\bar{\rho} = 0.95$. In the latter case, NACKs may be due to collisions.

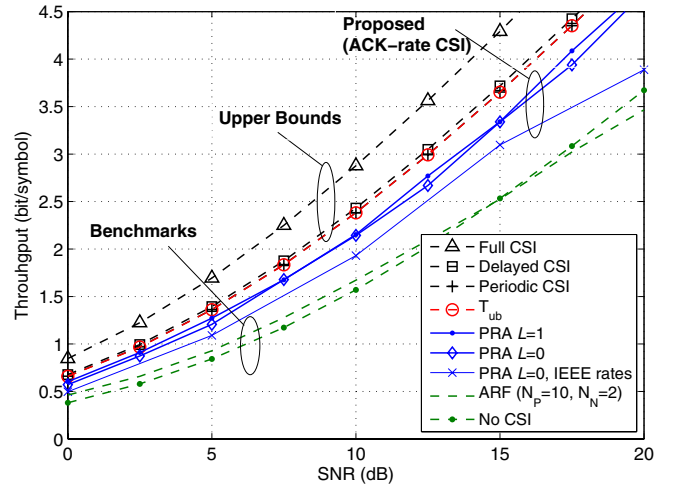


Fig. 7. The PRA compared to the benchmarks and upper bound. Parameters: $\bar{\rho} = 0.99$, $q_{10} = 0$, $q_{01} = 1$.

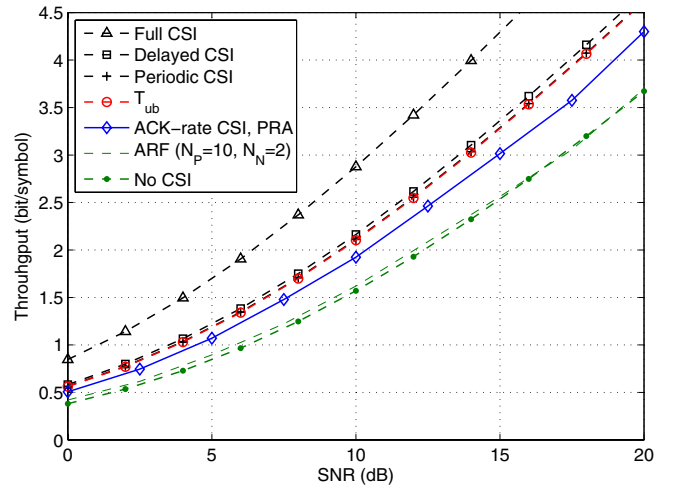


Fig. 8. The PRA compared to the benchmarks and upper bound. Parameters: $\bar{\rho} = 0.95$, $q_{10} = 0$, $q_{01} = 1$.

As mentioned in Section II, the PRA can account for collision and behave differently if collisions are present.

In Figs. 7–10, we employ Monte Carlo simulations to obtain the long-term throughput for ACK-rate CSI. We average the instantaneous throughput from packet $k = 100$ (after steady state) to packet $k = 1000$, then average again over 200 simulation runs. On the other hand, the maximum achievable throughput for other CSI is calculated analytically according to Section III-C. We vary $\bar{\gamma}$ over the practical range of 0 dB to 20 dB.

We consider the case of either no collision ($q_{10} = 0$, $q_{01} = 1$) or collision ($q_{10} = 0.4$, $q_{01} = 0.9$), and either moderate fading ($\bar{\rho} = 0.95$) or slow fading ($\bar{\rho} = 0.99$). To make numerical comparisons, we consider the difference in SNR (in dB) of two schemes to achieve a throughput of 2 bit/symbol.

1) *No Collision, Slow Fading*: From Fig. 7, the maximum achievable throughput T_{delayed}^* for delayed CSI incurs an SNR loss of around 2 dB compared to T_{full}^* for full CSI. This fundamental loss results from the temporal variation of the channel and the causality constraint imposed in practice, and

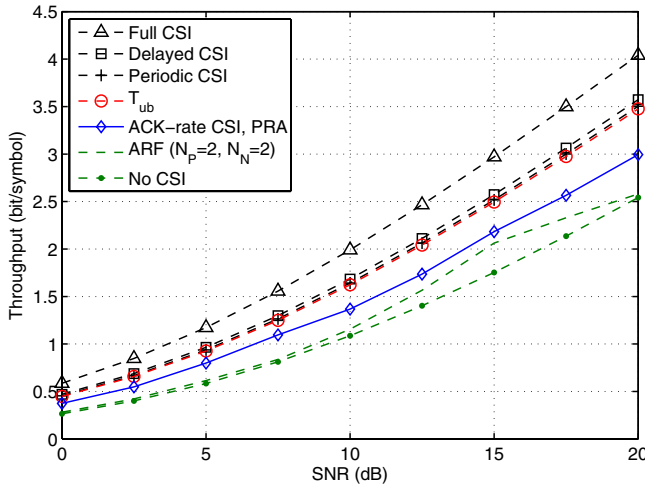


Fig. 9. The PRA compared to the benchmarks and upper bound. Parameters: $\bar{\rho} = 0.99$, $q_{10} = 0.4$, $q_{01} = 0.9$.

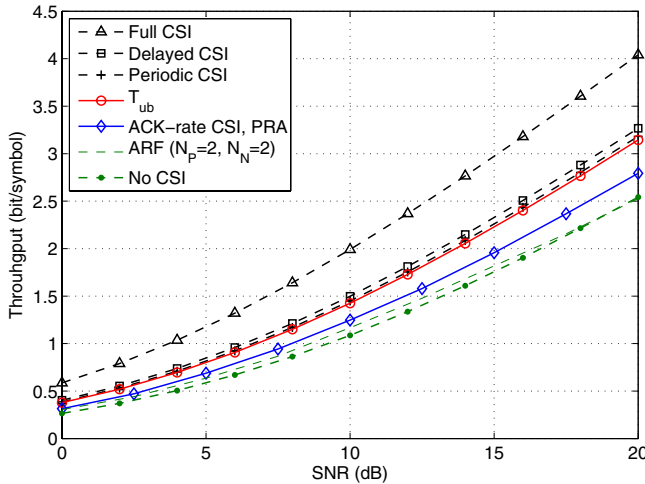


Fig. 10. The PRA compared to the benchmarks and upper bound. Parameters: $\bar{\rho} = 0.95$, $q_{10} = 0.4$, $q_{01} = 0.9$.

is irrecoverable. Moreover, $\mathcal{T}_{\text{delayed}}^*$ serves as an upper bound for $\mathcal{T}_{\text{ACK}}^*$ which cannot be directly computed. We also see that both new upper bounds $\mathcal{T}_{\text{periodic}}^*$, \mathcal{T}_{ub} are tighter than $\mathcal{T}_{\text{delayed}}^*$ by about 0.2 dB.

Fig. 7 also shows that the myopic policy with ACK-rate CSI, implemented by PRA with $L = 0$, is about one dB away from the tightest upper bound. This implies that the myopic policy cannot be more than one dB away from the optimal policy for ACK-rate CSI. Furthermore, we see that using $L = 1$, compared to using $L = 0$, improves the performance by a few tenths of dB at some SNRs. At low SNR, in particular, the performance becomes very close to the upper bound. Increasing L moderately (say $L = 2, 3, 4$) is not likely to bring about significant gain, but the complexity would already be prohibitive. Subsequently, we focus on the myopic policy where $L = 0$.

Generally, the maximum achievable throughput $\mathcal{T}_{\text{no}}^*$ for no CSI serves as a benchmark. We also consider the auto-rate fallback (ARF) scheme [16] as another benchmark. In the ARF scheme, the rate is increased after N_P consecutive PACKS and decreased after N_N consecutive NACKS. In the

Scenario: Collision, Fading speed	Gap to upper bound \mathcal{T}_{ub}	Gap to benchmark $\mathcal{T}_{\text{no}}^*$
No, Slow	1 dB (0.2 dB)	3 dB
No, Moderate	1 dB (0.3 dB)	2 dB
Yes, Slow	1.75 dB (0.4 dB)	2.6 dB
Yes, Moderate	1.5 dB (0.4 dB)	1.5 dB

TABLE II
SUMMARY OF THE PERFORMANCE OF PRA USING MYOPIC OPTIMIZATION, IN TERMS OF THE DIFFERENCE IN SNR TO ACHIEVE A THROUGHPUT OF 2 BIT/SYMBOL. THE IMPROVEMENT IN THE UPPER BOUND COMPARED TO $\mathcal{T}_{\text{delayed}}^*$ IS GIVEN WITHIN THE BRACKETS.

ARF scheme, only past ACKs, but not past rates, are used as CSI. We conducted a search by simulations to optimize N_P, N_N , where the optimized values are shown in the legend. Incidentally, for this no-collision slow-fading scenario, the optimized values of $N_P = 10, N_N = 2$ are the same as those considered in [16]. From Fig. 7, we observe that the PRA that exploits ACK-rate CSI performs significantly better than both benchmarks. For example, the PRA requires at least 3.1 dB less SNR at a throughput of 2 bit/symbol compared to $\mathcal{T}_{\text{no}}^*$. Some rate adaptation policies achieves higher throughput with more extensive or informative CSI, e.g., [6]–[8] which exploit the RTS/CTS mechanism, but they consume more channel resources than ACK feedback and so may not be suitable as benchmarks.

Finally, we investigate the degradation of using a smaller set of rates for adaptation, as available in IEEE 802.11a, i.e., $\mathcal{S}_R = \{0.5, 0.75, 1, 1.5, 2, 3, 4, 4.5\}$ bit/symbol. The channel state space \mathcal{S}_H remains unchanged. Rate adaptation is performed using the PRA with $L = 0$. Fig. 7 shows that the performance has degraded⁵ by about 1 dB at low SNR. At high SNR, the degradation becomes more significant. This suggests that, from the perspective of rate adaptation, the throughput of IEEE 802.11a may be further improved, especially at high SNR, by increasing the set of available rates.

2) *No Collision, Moderate Fading*: Fig. 8 shows that the throughput typically reduces when the speed of fading increases. Clearly, $\mathcal{T}_{\text{full}}^*$ is not affected as full CSI is available. However, $\mathcal{T}_{\text{delayed}}^*$ now incurs an additional SNR loss of around 1 dB compared to slow fading. We observe that both the proposed upper bounds $\mathcal{T}_{\text{periodic}}^*$ and \mathcal{T}_{ub} are tighter than $\mathcal{T}_{\text{delayed}}^*$ by about 0.3 dB.

3) *Collisions, Slow and Moderate Fading*: From Fig. 9 (slow fading) and Fig. 10 (moderate fading), the throughput is generally further reduced due to collisions. According to Theorem 1, this reduction is $p(\epsilon = 0) \approx 30\%$ for $\mathcal{T}_{\text{full}}^*$, $\mathcal{T}_{\text{delayed}}^*$, $\mathcal{T}_{\text{no}}^*$. The new upper bound \mathcal{T}_{ub} tightens $\mathcal{T}_{\text{delayed}}^*$ by about 0.4 dB.

The performance of the myopic policy with ACK-rate CSI, i.e., the PRA with $L = 0$, is summarized in Table II. We compare the PRA to the tightest upper bound \mathcal{T}_{ub} and to the benchmark $\mathcal{T}_{\text{no}}^*$, and also show the amount of tightening of the upper bound. Although this PRA is only optimal in a myopic sense, it is within 1 – 1.5 dB to the maximum achievable throughput and can improve performance by at least 1.5 dB, at a throughput of 2 bit/symbol. These results suggest that the

⁵The upper bounds and the benchmarks would also degrade accordingly. We omit the corresponding graphs for clarity of presentation.

PRA may be a good pragmatic approach for rate adaptation, especially for slowly fading channels with a low probability of collision.

VII. CONCLUSION

We have considered packet-by-packet rate adaptation to improve the average throughput over an infinite-time horizon, based on past ACKs and past rates as partial channel state information. We have taken collisions into account in our Markovian channel. Since the maximum achievable throughput cannot be practically computed, we have proposed two new upper bounds. We have shown that the myopic policy, which maximizes only the current throughput, achieves a throughput that is within one dB of the tightest upper bound over a wide range of SNRs for a slowly time-varying channel. This result suggests that the myopic policy is already fairly close to the maximum achievable throughput, yet at a reasonable complexity. Further, the particle filter is proposed to maintain the belief states necessary for throughput optimization. By using the particle-filter-based rate adaptation (PRA), the behavior of the rate adaptation process was studied by assuming availability of a large set of rates. This set of rates may be suitably pruned to simplify implementation.

The formulations and approaches used in this paper may be extended to other types of CSIs, e.g., when an additional quantized feedback of the channel state is available, so as to account for other feedback schemes used in practice. In our study, we assumed the parameters that described the long-term channel statistics are fixed and known. In practice, the parameters may not be exactly known or fluctuate over time. This necessitates an online estimation of the parameters which can be another interesting direction for further research.

ACKNOWLEDGEMENTS

The authors thank Jan Bergmans, Ludo Tolhuizen and Hongming Yang for helpful discussions. The authors also thank the anonymous reviewers for their helpful comments. Our inclusion of collision in this paper is based on the suggestion of one of the reviewers.

APPENDIX A AN AUXILIARY LEMMA

We state an auxiliary lemma that will be used in the proof of Lemma 5 and Theorem 3.

Lemma 3: Consider random variables X, Y, \tilde{H} which form a Markov chain $X \rightarrow Y \rightarrow \tilde{H}$, i.e., $p(X, Y, \tilde{H})$ can be factorized as $p(X)p(Y|X)p(\tilde{H}|Y)$. Then, the maximum expected value of an objective function $f(R, \tilde{H})$ obtained by optimizing R is larger given Y than given X , i.e.,

$$\mathbb{E}_Y \left[\max_R \mathbb{E}_{\tilde{H}|Y} [f(R, \tilde{H})] \right] \geq \mathbb{E}_X \left[\max_R \mathbb{E}_{\tilde{H}|X} [f(R, \tilde{H})] \right]. \quad (37)$$

Proof of Lemma 3: The operator $\mathbb{E}_{\tilde{H}|X}$ is equivalent to $\mathbb{E}_{Y|X} \mathbb{E}_{\tilde{H}|X, Y}$, while $\mathbb{E}_{\tilde{H}|X, Y}$ can be replaced by $\mathbb{E}_{\tilde{H}|Y}$ due to $X \rightarrow Y \rightarrow \tilde{H}$. Thus, the R.H.S of (37) can be written as

$$\begin{aligned} & \mathbb{E}_X \left[\max_R \mathbb{E}_{Y|X} \mathbb{E}_{\tilde{H}|Y} \left[f(R, \tilde{H}) \right] \right] \\ & \leq \mathbb{E}_X \mathbb{E}_{Y|X} \left[\max_R \mathbb{E}_{\tilde{H}|Y} \left[f(R, \tilde{H}) \right] \right] \\ & = \mathbb{E}_Y \left[\max_R \mathbb{E}_{\tilde{H}|Y} \left[f(R, \tilde{H}) \right] \right]. \end{aligned}$$

The inequality arises from interchanging the \max_R and $\mathbb{E}_{Y|X}$ operators, as $\max_R \sum_i p_i g(R) \leq \sum_i p_i \max_R g(R)$ for non-negative p_i and some function g . This thus proves (37). ■

Lemma 3 has an intuitive interpretation. Given $X \rightarrow Y \rightarrow \tilde{H}$, Y can be said to be more informative than X in describing \tilde{H} . Taking f as the throughput function, we interpret Lemma 3 to say that a myopic policy achieves a higher expected throughput with more informative CSI.

APPENDIX B PROOF OF THEOREM 2

Lemmas 4, 5, 6 below provide an ordering of the maximum achievable throughput for different CSIs, hence establishing Theorem 2.

Lemma 4: Let $\mathcal{T}_{\text{any}}^*$ be the maximum achievable throughput for any type of CSI. Then, $\mathcal{T}_{\text{full}}^* \geq \mathcal{T}_{\text{any}}^* \geq \mathcal{T}_{\text{no}}^*$. Consequently, $\mathcal{T}_{\text{full}}^* \geq \mathcal{T}_{\text{delayed}}^* \geq \mathcal{T}_{\text{no}}^*$.

Proof: Clearly $T(R_k; C_k) = \mathbb{E}_{\tilde{H}_k | C_k} [t(R_k, \tilde{H}_k)] \leq \mathbb{E}_{\tilde{H}_k | C_k} [\max_{R_k} t(R_k, \tilde{H}_k)]$ for any CSI C_k and rate R_k . Taking the expectation over C_k , we get $\mathbb{E}_{C_k} [T(R_k; C_k)] \leq \mathbb{E}_{\tilde{H}_k} [\max_{R_k} t(R_k, \tilde{H}_k)] = \mathcal{T}_{\text{full}}^*$ due to (14b). From (12), we thus get $\mathcal{T}(\pi) \leq \mathcal{T}_{\text{full}}^*$ for any policy π given any CSI. Then, maximizing $\mathcal{T}(\pi)$ over all policies establishes $\mathcal{T}_{\text{any}}^* \leq \mathcal{T}_{\text{full}}^*$. To see that $\mathcal{T}_{\text{any}}^* \geq \mathcal{T}_{\text{no}}^*$, we note that a policy given any CSI can always choose not to use the CSI and achieve $\mathcal{T}_{\text{no}}^*$, hence using the CSI optimally can only achieve the same or greater throughput. This completes the proof. ■

We say a CSI C_k at time k is *causal* if $C_k \rightarrow \tilde{H}_{k-1} \rightarrow \tilde{H}_k$. Thus, ACK-rate CSI, delayed CSI, periodic CSI and no CSI are all causal.

Lemma 5: The throughput achieved by a myopic policy with causal CSI C_k is no more than $\mathcal{T}_{\text{delayed}}^*$, i.e.,

$$\mathbb{E}_{C_k} \left[\max_R T(R; C_k) \right] \leq \mathcal{T}_{\text{delayed}}^*. \quad (38)$$

Consequently, $\mathcal{T}_{\text{delayed}}^* \geq \mathcal{T}_{\text{periodic}}^*$.

Proof: We know from Theorem 1 that $\mathcal{T}_{\text{delayed}}^*$ is achieved by a myopic policy. Since $C_k \rightarrow \tilde{H}_{k-1} \rightarrow \tilde{H}_k$, (38) follows immediately by applying Lemma 3 in Appendix A by defining the objective function f as the throughput t in (8), and random variables x, y, \tilde{H} as $C_k, \tilde{H}_{k-1}, \tilde{H}_k$, respectively. To show $\mathcal{T}_{\text{periodic}}^* \leq \mathcal{T}_{\text{delayed}}^*$, from the definition (23) with periodic CSI \hat{C}_k we get

$$\mathcal{T}_{\text{periodic}}^*(\pi) = \frac{1}{P} \max_{\pi} \mathbb{E} \left[\sum_{k=1}^P T(R_k; \hat{C}_k) \right] \quad (39)$$

$$\leq \frac{1}{P} \mathbb{E} \left[\sum_{k=1}^P \max_{R_k} T(R_k; \hat{C}_k) \right]. \quad (40)$$

Here, the inequality arises from interchanging the \max_{π} and \mathbb{E} operators. We have also replaced \max_{π} by \max_{R_k} in (40), since the rate R_k in π now optimizes each T separately given \hat{C}_k . Finally, since \hat{C}_k is causal, by applying (38) we obtain $\mathcal{T}_{\text{periodic}}^* \leq \mathcal{T}_{\text{delayed}}^*$. ■

Lemma 6: $\mathcal{T}_{\text{periodic}}^* \geq \mathcal{T}_{\text{ACK}}^*$.

Proof: In addition to the ACK-rate CSI, the periodic CSI is given by the periodic update of a delayed channel amplitude

at $k \in \mathcal{S}_P$. A policy given periodic CSI can always choose not to use this additional CSI and yet achieves $\mathcal{T}_{\text{ACK}}^*$. Using the periodic CSI optimally can only achieve the same or greater throughput, hence $\mathcal{T}_{\text{periodic}}^* \geq \mathcal{T}_{\text{ACK}}^*$. ■

APPENDIX C PROOF OF THEOREM 3

We note that to obtain \mathcal{T}_{ub} , the CSI used is causal and moreover only the throughput of the current packet k is maximized. Hence, Lemma 5 applies. From (38), we thus obtain $\mathcal{T}_{\text{delayed}}^* \geq \mathcal{T}_{\text{ub}}$. We now show that $\mathcal{T}_{\text{ub}} \geq \mathcal{T}_{\text{ACK}}^*$. From (12) and (13), we can write

$$\mathcal{T}_{\text{ACK}}^* = \lim_{K \rightarrow \infty} \frac{1}{K} \sum_{k=1}^K \mathbb{E}_{C_k^*} [T(R_k^*; C_k^*)] \quad (41)$$

where R_k^* denotes the rate selected by the optimal deterministic policy π^* , and

$$C_k^* = \{R_1^*, \dots, R_{k-1}^*, A_1^*, \dots, A_{k-1}^*\}$$

denotes the ACK-rate CSI that has a distribution resulting from the use of π^* . Each summand in (41) can be written as

$$\begin{aligned} & \mathbb{E}_{C_k^*} [T(R_k^*; C_k^*)] \\ &= \mathbb{E}_{C_k^*} \mathbb{E}_{\tilde{H}_k | C_k^*} \left[t(R_k^*, \tilde{H}_k) \right] \end{aligned} \quad (42a)$$

$$\leq \mathbb{E}_{C_k^*} \left[\max_{R_k} \mathbb{E}_{\tilde{H}_k | C_k^*} \left[t(R_k, \tilde{H}_k) \right] \right] \quad (42b)$$

$$\leq \mathbb{E}_{\tilde{C}_k^*} \left[\max_{R_k} \mathbb{E}_{\tilde{H}_k | \tilde{C}_k^*} \left[t(R_k, \tilde{H}_k) \right] \right] \quad (42c)$$

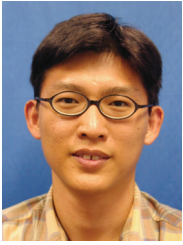
$$= \mathbb{E}_{\tilde{H}_{k-2}} \mathbb{E}_{R_{k-1}^*, A_{k-1}^* | \tilde{H}_{k-2}} \max_{R_k} T(R_k; \tilde{C}_k^*) \quad (42d)$$

$$\leq \mathbb{E}_{\tilde{H}_{k-2}} \max_{R_{k-1}} \mathbb{E}_{A_{k-1} | \tilde{H}_{k-2}} \left[\max_{R_k} T(R_k; \tilde{C}_k^*) \right] = \mathcal{T}_{\text{ub}}, \quad (42e)$$

where $\tilde{C}_k^* \triangleq \{R_{k-1}^*, A_{k-1}^*, \tilde{H}_{k-2}\}$. Here, (42a) follows the definition (9); (42b) follows from replacing R_k^* as a variable R_k to be optimized, given C_k^* ; (42c) follows from Lemma 3 in Appendix A, since it can be shown that $C_k^* \rightarrow \tilde{C}_k^* \rightarrow \tilde{H}_k$; (42d) follows directly from the definition of \tilde{C}_k^* and (9). Finally, (42e) follows from replacing (R_{k-1}^*, A_{k-1}^*) as a pair of variables (R_{k-1}, A_{k-1}) to be optimized given \tilde{H}_{k-2} , but since A_{k-1} depends only on R_{k-1} (given \tilde{H}_{k-2}), it is sufficient to optimize only R_{k-1} . In (42e), \tilde{C}_k^* is thus replaced by $\tilde{C}_k = \{R_{k-1}, A_{k-1}, \tilde{H}_{k-2}\}$. As (42e) in fact equals \mathcal{T}_{ub} in (19) by definition, it follows that each summand in (41) is no greater than \mathcal{T}_{ub} . Thus, $\mathcal{T}_{\text{ACK}}^* \leq \mathcal{T}_{\text{ub}}$. This concludes the proof.

REFERENCES

- [1] *Part 11: Wireless LAN Medium Access Control (MAC) and Physical Layer (PHY) Specifications*, IEEE 802.11 Standard, 1999.
- [2] *Evolved Universal Terrestrial Radio Access (E-UTRA): Physical channels and modulation*, 3GPP Std. 3GPP TS 36.211, Rev. 8.0.0, Sept. 2007. [Online]. Available: <http://www.3gpp.org/ftp/Specs/htmlinfo/36211.htm>
- [3] J. M. Wozencraft and M. Horstein, "Coding for two-way channels," Res. Lab. Electron., MIT, Cambridge, MA, Tech. Rep. 383, Jan. 1961.
- [4] P. Sindhu, "Retransmission error control with memory," *IEEE Trans. Commun.*, vol. 25, no. 5, pp. 473-479, May 1977.
- [5] G. Holland, N. Vaidya, and P. Bahl, "A rate-adaptive MAC protocol for multi-hop wireless networks," in *Proc. ACM MOBICOM'01*, July 2001, pp. 236-251.
- [6] S. H. Y. Wong, S. Lu, H. Yang, and V. Bharghavan, "Robust rate adaptation for 802.11 wireless networks," in *Proc. ACM MOBICOM'06*, 2006, pp. 146-157.
- [7] J. Kim, S. Kim, S. Choi, and D. Qiao, "CARA: Collision-aware rate adaptation for IEEE 802.11 WLANs," in *Proc. INFOCOM'06*, Apr. 2006, pp. 1-11.
- [8] B. Sadeghi, V. Kanodia, A. Sabharwal, and E. Knightly, "Opportunistic media access for multirate ad hoc networks," in *Proc. ACM MOBICOM'02*, 2002, pp. 24-35.
- [9] D. L. Goeckel, "Adaptive coding for time-varying channels using outdated fading estimates," *IEEE Trans. Commun.*, vol. 47, no. 6, pp. 844-855, June 1999.
- [10] Q. Liu, S. Zhou, and G. Giannakis, "Cross-layer combining of adaptive modulation and coding with truncated ARQ over wireless links," *IEEE Trans. Wireless Commun.*, vol. 3, no. 5, pp. 1746-1755, Sept. 2004.
- [11] H. Holma and A. Toskala, Eds., *HSDPA/HSUPA for UMTS: High Speed Radio Access for Mobile Communications*. West Sussex, England: Wiley, 2006.
- [12] J. del Prado Pavon and S. Choi, "Link adaptation strategy for IEEE 802.11 WLAN via received signal strength measurement," in *Proc. IEEE ICC '03*, vol. 2, Anchorage, AK, May 2003, pp. 1108-1113.
- [13] D. Qiao, S. Choi, and K. Shin, "Goodput analysis and link adaptation for IEEE 802.11a wireless LANs," *IEEE Trans. on Mobile Computing*, vol. 1, no. 4, pp. 278-292, Oct.-Dec. 2002.
- [14] P. Chevillat, J. Jelitto, A. N. Barreto, and H. L. Truong, "A dynamic link adaptation algorithm for IEEE 802.11a wireless LANs," in *Proc. IEEE ICC'03*, Anchorage, May 2003, pp. 1141-1145.
- [15] D. Qiao and S. Choi, "Fast-responsive link adaptation for IEEE 802.11 WLANs," in *Proc. IEEE ICC'05*, Seoul, Korea, May 2005, pp. 3583-3588.
- [16] A. Kamerman and L. Monteban, "WaveLAN-II: A high-performance wireless LAN for the unlicensed band," *Bell Labs Tech. J.*, pp. 118-133, Summer 1997.
- [17] M. Rice and S. B. Wicker, "Adaptive error control for slowly varying channels," *IEEE Trans. Commun.*, vol. 42, no. 234, pp. 917-926, Feb./Mar./Apr. 1994.
- [18] A. K. Karmokar, D. V. Djonin, and V. K. Bhargava, "POMDP-based coding rate adaptation for type-I hybrid ARQ systems over fading channels with memory," *IEEE Trans. Wireless Commun.*, vol. 5, no. 12, pp. 3512-3523, Dec. 2006.
- [19] C. H. Papadimitriou and J. N. Tsitsiklis, "The complexity of Markov decision processes," *Mathematics Operations Research*, vol. 12, no. 3, pp. 441-450, 1987.
- [20] C. C. Tan and N. C. Beaulieu, "On first-order Markov modeling for the Rayleigh fading channels," *IEEE Trans. Commun.*, vol. 48, no. 12, pp. 2032-2040, Dec. 2000.
- [21] N. Gordon, D. Salmund, and A. F. M. Smith, "Novel approach to nonlinear/non-Gaussian Bayesian state estimation," *Rad. Signal Processing, IEE Proc. F*, vol. 140, no. 2, pp. 107-113, Apr. 1993.
- [22] J. D. J. Costello, J. Hagenauer, H. Imai, and S. B. Wicker, "Applications of error-control coding," *IEEE Trans. Inform. Theory*, vol. 44, no. 6, pp. 2531-2560, Oct. 1998.
- [23] C. C. Tan and N. C. Beaulieu, "Infinite series representations of the bivariate Rayleigh and Nakagami-m distributions," *IEEE Trans. Commun.*, vol. 45, no. 10, pp. 1159-1161, Oct. 1997.
- [24] T. van Berkel, J.-P. Linnartz, and C. K. Ho, "Compensated estimators for characterizing interference in a Rayleigh fading environment," in *Proc. IEEE Symp. Commun. Veh. Technol. Benelux*, Delft, The Netherlands, Nov. 2007, pp. 1-4.
- [25] T. P. Minka, "From hidden Markov models to linear dynamical systems," Tech. Rep., revised 7/18/99.
- [26] J. Pearl, *Causality: Models, Reasoning, and Inference*. Cambridge, U.K.: Cambridge University Press, 2000.
- [27] D. P. Bertsekas, *Dynamic Programming and Optimal Control Vol. 1*. Belmont, MA: Athena Scientific, 1995.
- [28] M. Littman, A. Cassandra, and L. Kaelbling, "Learning policies for partially observable environments: scaling up," in *Proc. International Conf. Machine Learning*, 1995, pp. 362-370.
- [29] M. S. Arulampalam, S. Maskell, N. Gordon, and T. Clapp, "A tutorial on particle filters for online nonlinear/non-Gaussian Bayesian tracking," *IEEE Trans. Signal Process.*, vol. 50, no. 2, pp. 174-188, Feb. 2002.



Chin Keong Ho Chin Keong Ho received the B.Eng. (first-class Honors) and M.Eng. degrees from the Department of Electrical Engineering, National University of Singapore in 1999 and 2001, respectively. Since 2001, he is with the Institute for Infocomm Research, Singapore. He took leave in 2004-2007 to work toward the Ph.D. degree at Eindhoven University of Technology, The Netherlands, during which he conducted joint research with Philips Research Laboratories, Eindhoven, The Netherlands. His research interest lies in adaptive

wireless communications and signal processing for multicarrier and space-time communications.



Job Oostveen Job Oostveen is a senior researcher at TNO information and communication technologies. His research is focused on propagation modelling, performance assessment, radio network planning and optimization of MIMO-OFDM-based mobile networks. Among others, he is involved in radio network standardization in 3GPP. Before joining TNO, he was affiliated with Philips Research, where his research was focused on signal processing for multimedia (mainly video watermarking and fingerprinting) and wireless communications (MIMO,

OFDM, 802.11n). Job Oostveen holds a Ph.D. and M.Sc. in applied mathematics of the universities of Groningen and Twente, respectively.



Jean-Paul Linnartz Jean-Paul Linnartz is a Senior Technology Director at Philips Research in Eindhoven, the Netherlands, where he is responsible for research in the domain of sensor networks and systems. Previously he headed security and connectivity research groups. He is also a part-time professor at Eindhoven University of Technology.

He joined Philips in 1995, initially to set up a research activity on digital rights management for multi-media content and security systems. He applied signal detection principles in the field of electronic watermarking, and he invented various attacks and security measures. He introduced a privacy-preserving method of biometric identification that prevents misuse of templates from data bases. He proposed algorithms to mitigate Doppler intercarrier interference in OFDM reception for NXP chip sets for mobile DVB television reception. He introduced coded light, which is a dimming scheme that allows the embedding of identifiers in light sources, to facilitate convenient control of illumination.

In 1992-1995, he was an Assistant Professor at The University of California at Berkeley. In 1993, he proposed and analyzed Multi-Carrier CDMA. From 1988-1991 and in 1994, he was Assistant and Associate Professor at Delft University of Technology, respectively. He received his Ph.D. (Cum Laude) from T.U. Delft in December 1991 and his M.Sc. (Cum Laude) from Eindhoven University of Technology in 1986. Prof. Linnartz holds 25 patents.